

# Cold nuclear matter effects and a modified form of the proximity approach

Reza Gharaei \*

*Department of Physics, Sciences Faculty, Hakim Sabzevari University  
P. O. Box 397, Sabzevar, Iran*

## Abstract

The influence of the cold nuclear matter effects on the Coulomb barriers and also on the fusion cross sections of 47 fusion reactions are systematically investigated within the framework of the proximity formalism. For this purpose, I modify the original version of this formalism (Prox. 77) using a new analytical form of the universal function which is formulated based on the double-folding model with three density-dependent versions of the M3Y-type interactions, namely DDM3Y1, CDM3Y3 and BDM3Y1. It is found that when the Prox. 77 potential is accompanied by each of the formulated universal functions, the agreement between the theoretical and experimental data of the barrier height and also the fusion cross section increase for our selected fusion systems. The present study also provides appropriate conditions to explore theoretically the variation effects of the NM incompressibility constant  $K$  on the calculated results caused by the Prox. 77 model. It is shown that the accuracy of this potential model for reproducing the experimental fusion data enhances by increasing the strength of this constant. A discussion is also presented about the role of various physical effects in the theoretical results of the proximity approach.

PACS number(s): 25.70.Jj, 24.10.-i

Keywords: Fusion reactions; Density-dependent interactions; Universal function; Proximity formalism

---

\*r.gharaei@hsu.ac.ir

## I. INTRODUCTION

In recent decades, the advantage of the theoretical and experimental tools in the context of nuclear fusion reactions have provided favorable conditions to analyze various physical aspects of such reactions. From the theoretical point of view, it has always been interesting to examine the influence of nuclear properties on the complete fusion channel of two interacting nuclei. One popular approach to evaluate role of these properties is the proximity formalism. The original version of this formalism has been introduced based on the "proximity force theorem" and marked as proximity 1977 (Prox. 77) [1]. As a consequence of the literatures, one can find out that the proximity formalism needs to be modified for achieving more accurate predictions from the empirical/experimental data of the fusion reactions. During the recent years, many efforts have been done to improve the theoretical predictions of this approach [2, 3, 4, 5, 6, 7, 8, 9] In those studies, the authors tried to analyze the influence of the physical properties such as the thermal effects of the compound nucleus [2, 3, 4, 5, 6], the deformation effects of the target and/or projectile [7, 8] and the surface tension effects of two approaching nuclei [9] on the fusion process.

I can refer to the saturation property of cold nuclear matter (NM) as an another important issue of nuclear systems. Within the theoretical frameworks such as the double-folding (DF) model [10, 11] which is accompanied by the density-dependent (DD) M3Y interactions [12], one can explore the role of this effect in the different fusion systems. It is well known that the original density-independent M3Y interaction failed to predict the correct saturation properties of a cold NM (central nucleon density  $\rho_0 \simeq 0.17 \text{ fm}^{-3}$  and nucleon binding energy  $B(\rho_0) \simeq 16\text{MeV}$ ). An explicit density dependence for this type of effective NN force reduces the strength of interactions and also allows to consider the mentioned properties. Within the Hartree-Fock approach [13], D. T. Khoa and coworkers introduced eight DD versions of the M3Y interactions which are based upon the G-matrix elements of the Paris NN potentials [14]. As a consequence of the literature, these generalized DD versions give the correct saturation properties for alpha+nucleus scattering or elastic scattering of light nuclei [12, 15], but with different values for corresponding NM incompressibility constants  $K$  ranging from

170 to 270 MeV. It should be noted that when the DD interactions are employed in the DF model generate the nuclear potentials which are too deep at small internuclear distances. This feature is not suitable to reproduce the physical phenomena such as the steep-falloff in the fusion cross sections at energies far below the Coulomb barrier. To cure this deficiency, the theoretical studies such as Refs. [16, 17, 18] suggest that this model must be modified by simulating the repulsive core effects. The proposed procedure can be useful to justify the surface diffuseness anomaly in the heavy-ions reactions [19].

On the one side, the systematic studies such as Refs. [20, 21, 22, 23] indicate that the Prox. 77 potential model overestimates the empirical data of the barrier height in different fusion reactions. Moreover, this potential model underestimates the measured fusion cross sections. On the other hand, it was noted earlier that the density-dependence effects in the NN interactions reduce the strength of such interactions. Therefore, in the present study, we have motivated to impose indirectly these effects on the proximity formalism and analyze role of them in the Coulomb barrier and the fusion cross sections caused by this formalism. Finally, we are interested to explore the importance of the effects of changing the constant of the cold NM incompressibility on the theoretical results of the proximity potential. To reach these aims, we initially calculate the nuclear potential based on the DF model which is accompanied by three versions of M3Y interactions, namely DDM3Y1, CDM3Y3 and BDM3Y1. Then, using these calculated nuclear potentials and also definition of the proximity potential the behavior of the universal function  $\Phi(s)$  versus the  $s$  parameter is systematically studied for 47 fusion reactions. To analyze the energy-dependence behavior of the fusion cross sections by considering the cold NM effects in the selected fusion systems, we employ the one-dimensional barrier penetration model (1D-BPM).

This paper is organized as follows. Section II gives the relevant details of the theoretical models used to calculate the interaction potential. Sec. III is devoted to the employed procedure for parameterization of the universal function. The role of the cold NM effects in the theoretical predictions of the Prox. 77 potential are also studied in this section. In Sec. IV a discussion is presented about the influence of different physical effects on the proximity potential. The conclusions drawn from the present analysis are given in Sec. V.

## II. THEORETICAL FRAMEWORKS FOR NUCLEUS-NUCLEUS POTENTIAL

It is well recognized that the interaction potential plays a key role in the theoretical studies of the fusion reactions. In fact, an appropriate potential model enables us to reproduce the experimental data of the fusion cross sections with good precision. Nowadays, the properties of the Coulomb interactions of two colliding nuclei are well understood. In contrast, the introduction of a comprehensive theoretical model for evaluating various aspects of the nuclear forces is still as a challenge. Nevertheless, several theoretical approaches are available to calculate the nuclear part of the total interaction potential. In the present work, the calculations of this part are performed using two efficient models DF and proximity potential.

### A. Double-folding approach

This model is commonly used to calculate the optical potential in the elastic scattering [10, 25, 26]. In recent years, it has also been employed to evaluate the strength of the nuclear interactions in different fusion systems, for example see Refs. [27, 28, 29]. Using this microscopic approach, the nuclear potential between two participant nuclei can be calculated by the sum of the strength of the NN interactions through a six-dimensional integral as

$$V_{\text{DF}}(\mathbf{R}) = \int d\mathbf{r}_1 \int d\mathbf{r}_2 \rho_1(\mathbf{r}_1) \rho_2(\mathbf{r}_2) v_{NN}(\mathbf{r}_{12} = \mathbf{R} + \mathbf{r}_2 - \mathbf{r}_1). \quad (1)$$

This relation reveals that the DF integral has two main inputs; one is the effective NN interaction  $v_{NN}$  and the other is the density distribution of the participant nuclei  $\rho_i(\mathbf{r}_i)$ . In the present study, the former part is parameterized by employing the M3Y-Paris [30] effective interaction with a finite range approximation for its exchange part. Moreover, for parametrization of the latter part we have used a two-parameter Fermi-Dirac (2PF) distribution function

$$\rho_{2\text{PF}}(r) = \frac{\rho_0}{1 + \exp[(r - R_0)/a_0]}, \quad (2)$$

Here,  $R_0$  and  $a_0$  are the radial and the diffuseness parameters of nucleus, respectively.

## B. Proximity approach

Proximity force theorem [1] predicts that two approaching surfaces interact with each other via the proximity force  $F(s)$  at the short distances within 2 to 3 fm. Under these conditions, one can evaluate the nuclear proximity potential using the following relation

$$F(s) = -\left(\frac{\partial V_N^{\text{Prox.}}}{\partial s}\right). \quad (3)$$

The final form of  $V_N^{\text{Prox.}}$  can be defined as a product of two functions. One is dependent on the shape and geometry of the interaction system  $f(\text{shap.}, \text{geom.})$  and the other is universal function  $\Phi(s)$ ,

$$V_N^{\text{Prox.77}}(r) = 4\pi\gamma b\overline{R} \Phi\left(\frac{s}{b}\right) \text{ MeV}, \quad (4)$$

where various parts of this relation are given as follows.

- The mean curvature radius  $\overline{R}$  is

$$\overline{R} = \frac{C_1 C_2}{C_1 + C_2}, \quad (5)$$

with

$$C_i = R_i \left[ 1 - \frac{b^2}{R_i^2} + \dots \right] \quad (i = 1, 2). \quad (6)$$

- The effective sharp radius  $R_i$  is

$$R_i = 1.28A_i^{1/3} - 0.76 + 0.8A_i^{-1/3} \text{ fm} \quad (i = 1, 2). \quad (7)$$

- The separation distance between the half-density surfaces of the nuclei  $s$  is

$$s = r - C_1 - C_2, \quad (8)$$

- The surface energy coefficient  $\gamma$  is

$$\gamma = \gamma_0 \left[ 1 - k_s \left( \frac{N - Z}{N + Z} \right)^2 \right] \text{ MeVfm}^{-2}, \quad (9)$$

where  $\gamma_0$  and  $k_s$  are 0.9517 MeV/fm<sup>2</sup> and 1.7826, respectively. Moreover,  $N$  and  $Z$  denote the neutron and proton numbers of the compound system.

- The universal function  $\Phi(\xi = s/b)$  of the original version of the proximity potential is

$$\Phi(\xi) = \begin{cases} -\frac{1}{2}(\xi - 2.54)^2 - 0.0852(\xi - 2.54)^3 & \text{for } \xi \leq 1.2511 \\ -3.437\exp(-\xi/0.75) & \text{for } \xi \geq 1.2511 \end{cases} \quad (10)$$

where  $b$  is of order of 1 fm.

### III. CALCULATIONS AND RESULTS

#### A. Parameterization of the universal function

As pointed before, we intend to investigate indirectly the cold NM effects on the fusion barriers caused by the Prox. 77 potential using the DD versions of the M3Y interactions. To address this goal, I select 47 symmetric and asymmetric fusion reactions with condition of  $48 \leq Z_1 Z_2 \leq 2460$  for charge product of their projectile and target. Our lightest reaction taken is that of  $^{12}\text{C} + ^{17}\text{O}$ , whereas the heaviest one is of  $^{70}\text{Zn} + ^{208}\text{Pb}$ . Moreover, it is assumed that all colliding nuclei to be spherical in nature.

Using Eq. (4), one can obtain the following expression for evaluating the universal function

$$\Phi(s) = \frac{V_N(s)}{4\pi\gamma\bar{R}b}. \quad (11)$$

Here, the nuclear potential  $V_N(s)$  is determined based upon the DF model which is accompanied by the DD versions of the M3Y-type forces. Since the ability of this approach is the prediction of the surface interactions in the regions of around the Coulomb barrier, the radial distance between the centers of the participant nuclei during the fusion process is restricted to  $-1 \leq s \leq 5$  range. Moreover, we employ the radial and diffuseness parameters presented in Table I to parameterize the density distribution functions of the reacting nuclei in the selected fusion systems. The values of these parameters are extracted from Refs. [27, 31].

The behavior of the calculated values of the universal function versus the parameter  $s$  have been analyzed for all considered fusion reactions in Fig. 1. The parts of (a), (b) and (c)

of this figure are devoted to the results of DF(DDM3Y1), DF(CDM3Y3) and DF(BDM3Y1) potential models, respectively. It is found that by increasing the values of  $s$  parameter in the considered fusion reactions and increasing the contribution of the surface interactions in the DF potential, the universal functions calculated by each of the mentioned versions tend to a certain constant value. In contrast, there are fairly significant deviations in the overlapping regions. Here, a nonlinear (fourth-order) function is used to parameterize the behavior of  $\Phi(s)$  as follows

$$\Phi(s) = b_0 + b_1s + b_2s^2 + b_3s^3 + b_4s^4 \quad (12)$$

where the values of the constant coefficients  $b_i$  are listed in Table II for each of the considered potential models.

The comparison of the present pocket formula with Eq. (10) demonstrates that the strength of the universal function becomes more negative by imposing the DD effects. This result is clear from Fig. 2. Moreover, since the radial behavior of the universal function is generally similar to the nuclear potential, the deviations of our pocket formula from Eq. (10) in the overlapping regions can be attributed to the intrinsic properties such as the repulsive core effects which have not been considered in the DF formalism. The variation effects of the cold NM incompressibility constant on the mentioned function is quite evident. In fact, by increasing the strength of this constant from  $K = 176$  MeV (in DDM3Y1 version) to  $K = 270$  MeV (in BDM3Y1 version), the strength of  $\Phi(s)$  reduces.

## B. Fusion barrier

Using the suggested form of the universal function, one can compute the strength of the nuclear proximity potential at various internuclear distances. Here, the modified forms of the Prox. 77 potential are labeled as "Prox.77(DDM3Y1)", "Prox.77(CDM3Y3)" and "Prox.77(BDM3Y1)". By adding a simple form of the Coulomb potential as  $V_C(r) = \frac{Z_1Z_2e^2}{r}$  to these modified nuclear potentials, the total interaction potentials can be calculated for our selected fusion systems. Fig. 3 shows the theoretical values of the barrier height  $V_B^{\text{Thero.}}$  as a function of the corresponding experimental data  $V_B^{\text{Exp.}}$  based on the Prox. 77 model and

also its modified forms. One can observe that the cold NM effects improve the agreement between the theoretical and experimental data of the barrier height for our selected mass range. Furthermore, this agreement enhances by increasing the strength of the incompressibility constant from Prox.77(DDM3Y1) model to Prox.77(BDM3Y1) one.

### C. Fusion cross section

Another right tool for investigating the complete fusion channel of two interaction nuclei is the fusion cross section. In the present study, 1D-BPM [32] is employed to calculate the theoretical values of this quantity. It is well known that in this model the separation distance of the reacting nuclei is considered as only degree freedom of the interaction system. Under these conditions, the fusion cross section  $\sigma_{\text{fus}}$  at center-of-mass energy  $E_{\text{c.m.}}$  can be defined by following relation

$$\sigma_{\text{fus}}(E_{\text{c.m.}}) = \frac{\pi \hbar^2}{2\mu E_{\text{c.m.}}} \sum_{\ell=0}^{\infty} (2\ell + 1) T_{\ell}(E_{\text{c.m.}}). \quad (13)$$

where  $\mu$  and  $T_{\ell}(E_{\text{c.m.}})$  are the reduced mass of the colliding system and the transmission coefficient through the fusion barrier, respectively. Using the WKB approximation [33], the dependence of this coefficient on the energy and the angular momentum quantities can be extracted as follows

$$T_{\ell}(E_{\text{c.m.}}) = \left[ 1 + \exp \left( 2 \sqrt{\frac{2\mu}{\hbar^2}} \int_{r_{1\ell}}^{r_{2\ell}} dr [V_0(r) + \frac{\hbar^2 \ell(\ell+1)}{2\mu r^2} - E_{\text{c.m.}}]^{1/2} \right) \right]^{-1}, \quad (14)$$

where  $r_{1\ell}$  and  $r_{2\ell}$  are classical turning points for angular momentum  $\ell$  and  $V_0(r)$  is total potential for  $\ell = 0$ .

The previous studies such as Refs. [20, 22, 23] reveal that the Prox. 77 potential underestimates the measured fusion cross sections at various barrier energies. Our investigation proves that the imposing of the cold NM effects on this potential reduces the fusion barrier height and resulting in one can expect that the calculated fusion cross sections enhance. Figure 4 confirms this result for four arbitrary colliding systems  $^{16}\text{O}+^{208}\text{Pb}$ ,  $^{40}\text{Ca}+^{40}\text{Ca}$ ,  $^{16}\text{O}+^{144}\text{Sm}$ ,  $^{16}\text{O}+^{72}\text{Ge}$ . In this figure the behavior of the calculated fusion cross sections  $\sigma_{\text{fus}}$



(in millibarns) are plotted as a function of  $E_{c.m.}$  energy (in MeV). It is shown that the Prox. 77 (DDM3Y1), Prox. 77 (CDM3Y3) and Prox. 77 (BDM3Y1) potential models predict separately the experimental data of the mentioned quantity with more accuracy than the Prox. 77 model. Moreover, among three modified proximity versions, the Prox. 77 (BDM3Y1) potential has the best consistent with the fusion data.

#### IV. COMPARISON WITH THE OTHER PHYSICAL EFFECTS

The systematic studies such as Refs. [24, 34, 37] reveal that the theoretical results caused by the proximity formalism can be improved by taking into account various corrective effects. In this section, the importance of those physical effects on the theoretical predictions of the Prox. 77 model will be compared with the cold NM effects for our selected mass range. To achieve further understanding, we calculate the percentage difference between the theoretical and experimental data of  $V_B$  using the following relation

$$\Delta V_B(\%) = \frac{V_B^{\text{Theor.}} - V_B^{\text{Exp.}}}{V_B^{\text{Exp.}}} \times 100. \quad (15)$$

The calculated values of  $\Delta V_B(\%)$  versus the charge product  $Z_1 Z_2$  are plotted in Fig. 5. We mark the results of the previous improved proximity models as IPM1 [34], IPM2 [37], IPM3 [24]. As a consequence, one can see that the discrepancy between the theoretical and experimental data of the barrier height reduces by imposing each of the considered effects on the Prox. 77 potential. The obtained values of chi-squared ( $\chi^2 = \frac{1}{N} \sum_{i=1}^N [V_B^{\text{Theor.}}(i) - V_B^{\text{Exp.}}(i)]^2$ ) based on the considered proximity potentials are listed in Table III. It is clearly visible from this table that the Prox. 77 (BDM3Y1) model reproduces the experimental data with more accuracy than the other modified versions. Indeed, the cold NM effects have the most important role in improving the calculated barrier heights for our fusion reactions.

It can be attractive to explore the importance of the above physical effects on the energy-dependent behavior of the fusion cross sections. The results of such evaluation have been shown in Fig. 6 for three arbitrary colliding systems  $^{35}\text{Cl} + ^{54}\text{Fe}$ ,  $^{16}\text{O} + ^{116}\text{Sn}$  and  $^{24}\text{Mg} + ^{35}\text{Cl}$ . As evident from this figure, all modified forms of the proximity potential are more successful

than the Prox. 77 model to reproduce the experimental data of  $\sigma_{\text{fus}}$ . Moreover, this figure reveals that the best results belongs to the proximity potential with the corrective effects of the cold NM.

## V. SUMMARY AND CONCLUSIONS

A systematic study of the cold NM effects, including the saturation, density and incompressibility properties, on the various characteristics of the complete fusion channel of 47 colliding systems is presented using the proximity formalism. We have introduced a parameterized form of the universal function  $\Phi(s)$  using the DF model with three DD versions of the M3Y-type forces. The quality of the original version of the proximity formalism which is modified with the parameterized form of  $\Phi(s)$  is explored for reproducing the experimental data of the barrier height and the fusion cross section of different fusion reactions. 1D-BPM is used to compute the theoretical values of the fusion cross section. The most important results of the present study can be summarized in what follows.

(i) The behavior of the universal function  $\Phi(s)$  against the  $s$  parameter reveals that the strength of this function reduces by increasing the strength of the incompressibility constant  $K$  in the DD versions of the M3Y interactions.

(ii) It is shown that the imposing of the DD effects in the proximity formalism improves the agreement between the theoretical and experimental data of  $V_B$ . Moreover, this agreement enhances by increasing the strength of the incompressibility constant  $K$  for our selected mass range. In other words, the Prox. 77 potential generates the best result for theoretical values of the barrier height in a hard NM.

(iii) The analysis of the energy-dependent behavior of the fusion cross sections illustrates that the Prox.77 (BDM3Y1) model significantly improves the calculated values of this quantity for my considered fusion reactions. In fact, the original version of the proximity formalism with the corrective effects of the hard nuclear matter incompressibility reproduces the experimental data of  $\sigma_{\text{fus}}$ , with more accuracy than the medium and soft ones.

(iv) The importance of the cold NM effects in the improvement of the theoretical pre-

dictions of the Prox. 77 model is compared with the other physical effects such as the temperature and  $\gamma$  coefficient effects. The obtained results confirm that the corrective effects of hard NM in comparison with those proposed in previous works [24, 34, 37] generate the more accurate results for barrier heights and fusion cross sections caused by the Prox. 77 model.

## References

- [1] J. Blocki, J. Randrup, W. J. Swiatecki and C. F. Tsang, Ann. Phys. (NY) **105**, 427 (1977).
- [2] R. Kumar, Phys. Rev. C **84**, 044613 (2011).
- [3] R. Kumar, M. Bansal, S. K. Arun and R. K. Gupta, Phys. Rev. C **80**, 034618 (2009).
- [4] O. N. Ghodsi and R. Gharaei, Phys. Rev. C **88**, 054617 (2013).
- [5] O. N. Ghodsi, H. R. Moshfegh and R. Gharaei, Phys. Rev. C **88**, 034601 (2013).
- [6] M. Salehi and O. N. Ghodsi, Chin. Phys. Lett. **30**, 042502 (2013).
- [7] D. Jain, R. Kumar and M. K. Sharma, Nucl. Phys. A **915**, 106 (2013).
- [8] O. N. Ghodsi and V. Zanganeh, Phys. Rev. C **79**, 044604 (2009).
- [9] I. Dutt and R. K. Puri, Phys. Rev. C **81**, 047601 (2010).
- [10] G. R. Satchler and W. G. Love, Phys. Rep. **55**, 183 (1979).
- [11] D. T. Khoa and G. R. Satchler, Nucl. Phys. A **668**, 3 (2000).
- [12] D. T. Khoa, G. R. Satchler and W. von Oertzen, Phys. Rev. C **56**, 954 (1997).
- [13] D. T. Khoa and W. von Oertzen, Phys. Lett. B **304**, 8 (1993).
- [14] N. Anantaraman, H. Toki and G. F. Bertsch, Nucl. Phys. A **398**, 269 (1983).
- [15] M. E. Brandan and G. R. Satchler, Phys. Rep. **285**, 143 (1997).
- [16] S. Misicu and H. Esbensen, Phys. Rev. Lett. **96**, 112701 (2006).
- [17] S. Misicu and H. Esbensen, Phys. Rev. C **75**, 034606 (2007).
- [18] E. Uegaki and Y. Abe, Prog. Theor. Phys. **90**, 615 (1993).

- [19] O. N. Ghodsi and V. Zanganeh, Nucl. Phys. A **846**, 40 (2010).
- [20] O. N. Ghodsi and R. Gharaei, Phys. Rev. C **88**, 054617 (2013).
- [21] I. Dutt and R. Bansal, Chin. Phys. Lett. **27**, 112402 (2010).
- [22] I. Dutt and R. K. Puri, Phys. Rev. C **81**, 044615 (2010).
- [23] I. Dutt and R. K. Puri, Phys. Rev. C **81**, 064609 (2010).
- [24] C. L. Guo, G. L. Zhang and X. Y. Le, Nucl. Phys. A **897**, 54 (2013).
- [25] C. W. Glover, R. I. Cutler and K. W. Kemper, Nucl. Phys. A **341**, 137 (1980).
- [26] M. E. Brandan and G. R. Satchler, Phys. Rep. **285**, 143 (1997).
- [27] I. I. Gontchar, D. J. Hinde, M. Dasgupta and J. O. Newton, Phys. Rev. C **69**, 024610 (2004).
- [28] M Rashdan, J. Phys. G: Nucl. Part. Phys. **22**, 139 (1996).
- [29] W M Seif, J. Phys. G: Nucl. Part. Phys. **30**, 1231 (2004).
- [30] G. Bertsch, J. Borysowicz, H. McManus and W. G. Love, Nucl. Phys. A **284**, 399 (1977).
- [31] H. de Vries, C. W. deJager and C. de Vries, At. Data Nucl. Data Tables **36**, 495 (1987).
- [32] A. B. Balantekin and N. Takigawa Reviews of Modern Physics, Vol. **70**, 77 (1998).
- [33] E. C. Kemble, Phys. Rev. **48**, 549 (1935).
- [34] M. Salehi and O. N. Ghodsi, Chin. Phys. Lett. **30**, 042502 (2013).
- [35] P. O. Biney, W. Dong and J. H. Lienhard, J. Heat Transfer, **108**, 405 (1986).
- [36] I. V. J. H. Lienhard and V. J. H. Lienhard, *A Heat Transfer Textbook* (Phlogiston Press), chap 9, p 465.
- [37] I. Dutt and R. K. Puri, Phys. Rev. C **81**, 047601 (2010).

- [38] C. R. Morton, A. C. Berriman, M. Dasgupta, D. J. Hinde, J. O. Newton, K. Hagino and I. J. Thompson, Phys. Rev. C **60**, 044608 (1999).
- [39] H. A. Aljuwair *et al.*, Phys. Rev. C **30**, 1223 (1984).
- [40] J. R. Leigh, M. Dasgupta, D. J. Hinde *et al.*, Phys. Rev. C **52**, 3151 (1995).
- [41] E. F. Aguilera, J. J. Kolata and R. J. Tighe, Phys. Rev. C **52**, 3103 (1995).
- [42] E. M. Szanto, R. Liguori Neto, M. C. S. Figueira *et al.*, Phys. Rev. C **41**, 2164 (1990).
- [43] V. Tripathi *et al.*, Phys. Rev. C **65**, 014614 (2001).
- [44] Sl. Cavallaro, M. L. Sperduto, B. Delaunay *et al.*, Nucl. Phys., A **513**, 174 (1990).

## FIGURE CAPTIONS

Fig. 1. The behavior of the universal function  $\Phi(s)$  versus the  $s$  parameter based on the (a) DF(DDM3Y1) (b) DF(CDM3Y3) and (c) DF(BDM3Y1) potential models.

Fig. 2. Dependence of the universal function on the variation effects of the NM incompressibility constant  $K$ . A comparison has also been performed with the analytical form suggested in Ref. [1].

Fig.3. The behavior of the theoretical barrier heights  $V_B^{\text{Theor.}}$  (in MeV) as a function of their corresponding experimental data  $V_B^{\text{Exp.}}$  (in MeV) based on the (a) Prox. 77, (b) Prox. 77 (DDM3Y1), (c) Prox. 77 (CDM3Y3) and (d) Prox. 77 (BDM3Y1) proximity potentials for present fusion reactions.

Fig. 4. Experimental fusion excitation functions for the systems (a)  $^{16}\text{O}+^{208}\text{Pb}$  [38], (b)  $^{40}\text{Ca}+^{40}\text{Ca}$  [39], (c)  $^{16}\text{O}+^{144}\text{Sm}$  [40] and (d)  $^{16}\text{O}+^{72}\text{Ge}$  [41] compared with theoretical predictions of the Prox. 77 model and its modified forms.

Fig. 5. The percentage differences between the theoretical and experimental data of the barrier height as a function of charge product  $Z_1Z_2$  for our selected mass range. They are calculated using the Prox. 77 potential and its modified forms.

Fig. 6. Role of various physical effects in the fusion cross sections based on the Prox. 77 for (a)  $^{35}\text{Cl}+^{54}\text{Fe}$  [42], (b)  $^{16}\text{O}+^{116}\text{Sn}$  [43] and (c)  $^{24}\text{Mg}+^{35}\text{Cl}$  [44] fusion reactions.

Table I. The radial ( $R_0$ ) and diffuseness ( $a_0$ ) parameters of various projectile and target nuclei of our selected reactions for parameterization of their density distribution functions in DF integral, Eq. (1). The systems are listed with respect to their increasing  $Z_1 Z_2$  values.

Nucleus	$Z_1 Z_2$	$R_{0(P)}$	$a_{0(P)}$	$R_{0(T)}$	$a_{0(T)}$
$^{12}\text{C}+^{17}\text{O}$	48	2.441 <sup>a</sup>	0.456 <sup>a</sup>	2.661 <sup>a</sup>	0.466 <sup>a</sup>
$^{16}\text{O}+^{16}\text{O}$	64	2.608 <sup>a</sup>	0.465 <sup>a</sup>	2.608 <sup>a</sup>	0.465 <sup>a</sup>
$^{16}\text{O}+^{40}\text{Ca}$	160	2.608 <sup>a</sup>	0.465 <sup>a</sup>	3.766 <sup>a</sup>	0.544 <sup>a</sup>
$^{26}\text{Mg}+^{30}\text{Si}$	168	3.05 <sup>b</sup>	0.523 <sup>b</sup>	3.252 <sup>b</sup>	0.553 <sup>b</sup>
$^{24}\text{Mg}+^{35}\text{Cl}$	204	2.980 <sup>b</sup>	0.551 <sup>b</sup>	3.476 <sup>a</sup>	0.559 <sup>a</sup>
$^{12}\text{C}+^{92}\text{Zr}$	240	2.441 <sup>a</sup>	0.456 <sup>a</sup>	4.913 <sup>a</sup>	0.533 <sup>a</sup>
$^{16}\text{O}+^{72}\text{Ge}$	256	2.608 <sup>a</sup>	0.465 <sup>a</sup>	4.450 <sup>b</sup>	0.573 <sup>b</sup>
$^{16}\text{O}+^{92}\text{Zr}$	320	2.608 <sup>a</sup>	0.465 <sup>a</sup>	4.913 <sup>a</sup>	0.533 <sup>a</sup>
$^{36}\text{S}+^{48}\text{Ca}$	320	3.509 <sup>a</sup>	0.560 <sup>a</sup>	3.7369 <sup>b</sup>	0.5245 <sup>b</sup>
$^9\text{Be}+^{208}\text{Pb}$	328	2.218 <sup>a</sup>	0.458 <sup>a</sup>	6.631 <sup>a</sup>	0.505 <sup>a</sup>
$^{19}\text{F}+^{93}\text{Nb}$	369	2.590 <sup>b</sup>	0.564 <sup>b</sup>	4.870 <sup>b</sup>	0.573 <sup>b</sup>
$^{12}\text{C}+^{152}\text{Sm}$	372	2.441 <sup>a</sup>	0.456 <sup>a</sup>	5.8044 <sup>b</sup>	0.581 <sup>b</sup>
$^{16}\text{O}+^{116}\text{Sn}$	400	2.608 <sup>a</sup>	0.465 <sup>a</sup>	5.538 <sup>b</sup>	0.550 <sup>b</sup>
$^{40}\text{Ca}+^{40}\text{Ca}$	400	3.766 <sup>a</sup>	0.544 <sup>a</sup>	3.766 <sup>a</sup>	0.544 <sup>a</sup>
$^{40}\text{Ca}+^{48}\text{Ca}$	400	3.766 <sup>a</sup>	0.544 <sup>a</sup>	3.7369 <sup>b</sup>	0.5245 <sup>b</sup>
$^{48}\text{Ca}+^{48}\text{Ca}$	400	3.7369 <sup>b</sup>	0.5245 <sup>b</sup>	3.7369 <sup>b</sup>	0.5245 <sup>b</sup>
$^{27}\text{Al}+^{70}\text{Ge}$	416	3.070 <sup>b</sup>	0.519 <sup>b</sup>	4.440 <sup>b</sup>	0.585 <sup>b</sup>
$^{40}\text{Ca}+^{48}\text{Ti}$	440	3.766 <sup>a</sup>	0.544 <sup>a</sup>	3.843 <sup>b</sup>	0.588 <sup>b</sup>
$^{35}\text{Cl}+^{54}\text{Fe}$	442	3.476 <sup>a</sup>	0.559 <sup>a</sup>	4.075 <sup>b</sup>	0.506 <sup>b</sup>
$^{12}\text{C}+^{204}\text{Pb}$	492	2.441 <sup>a</sup>	0.456 <sup>a</sup>	6.588 <sup>a</sup>	0.504 <sup>a</sup>
$^{16}\text{O}+^{144}\text{Sm}$	496	2.608 <sup>a</sup>	0.465 <sup>a</sup>	5.719 <sup>a</sup>	0.557 <sup>a</sup>
$^{16}\text{O}+^{148}\text{Sm}$	496	2.608 <sup>a</sup>	0.465 <sup>a</sup>	5.771 <sup>b</sup>	0.596 <sup>b</sup>
$^{17}\text{O}+^{144}\text{Sm}$	496	2.661 <sup>a</sup>	0.466 <sup>a</sup>	5.719 <sup>a</sup>	0.557 <sup>a</sup>
$^{28}\text{Si}+^{92}\text{Zr}$	560	3.140 <sup>b</sup>	0.537 <sup>b</sup>	4.913 <sup>a</sup>	0.533 <sup>a</sup>
$^{32}\text{S}+^{89}\text{Y}$	624	3.374 <sup>a</sup>	0.558 <sup>a</sup>	4.760 <sup>b</sup>	0.571 <sup>b</sup>
$^{34}\text{S}+^{89}\text{Y}$	624	3.443 <sup>a</sup>	0.559 <sup>a</sup>	4.760 <sup>b</sup>	0.571 <sup>b</sup>
$^{36}\text{S}+^{90}\text{Zr}$	640	3.509 <sup>a</sup>	0.560 <sup>a</sup>	4.878 <sup>a</sup>	0.532 <sup>a</sup>
$^{36}\text{S}+^{96}\text{Zr}$	640	3.509 <sup>a</sup>	0.560 <sup>a</sup>	4.922 <sup>a</sup>	0.533 <sup>a</sup>
$^{16}\text{O}+^{208}\text{Pb}$	656	2.608 <sup>a</sup>	0.465 <sup>a</sup>	6.631 <sup>a</sup>	0.505 <sup>a</sup>
$^{35}\text{Cl}+^{92}\text{Zr}$	680	3.476 <sup>a</sup>	0.559 <sup>a</sup>	4.913 <sup>a</sup>	0.533 <sup>a</sup>
$^{16}\text{O}+^{186}\text{W}$	700	2.608 <sup>a</sup>	0.465 <sup>a</sup>	6.580 <sup>b</sup>	0.480 <sup>b</sup>
$^{19}\text{F}+^{197}\text{Au}$	711	2.590 <sup>b</sup>	0.564 <sup>b</sup>	6.380 <sup>b</sup>	0.535 <sup>b</sup>
$^{16}\text{O}+^{238}\text{U}$	736	2.608 <sup>a</sup>	0.465 <sup>a</sup>	6.8054 <sup>b</sup>	0.605 <sup>b</sup>

(a) Based on the 2PF profile extracted from [27]

(b) Based on the 2PF profile extracted from [31]



Table I. (Continued.)

Nucleus	$Z_1 Z_2$	$R_{0(P)}$	$a_{0(P)}$	$R_{0(T)}$	$a_{0(T)}$
$^{19}\text{F} + ^{208}\text{Pb}$	738	2.590 <sup>b</sup>	0.564 <sup>b</sup>	6.631 <sup>a</sup>	0.505 <sup>a</sup>
$^{40}\text{Ca} + ^{90}\text{Zr}$	800	3.766 <sup>a</sup>	0.544 <sup>a</sup>	4.878 <sup>a</sup>	0.532 <sup>a</sup>
$^{40}\text{Ca} + ^{96}\text{Zr}$	800	3.766 <sup>a</sup>	0.544 <sup>a</sup>	4.922 <sup>a</sup>	0.533 <sup>a</sup>
$^{32}\text{S} + ^{116}\text{Sn}$	800	3.374 <sup>a</sup>	0.558 <sup>a</sup>	5.358 <sup>b</sup>	0.550 <sup>b</sup>
$^{28}\text{Si} + ^{144}\text{Sm}$	868	3.140 <sup>b</sup>	0.537 <sup>b</sup>	5.719 <sup>a</sup>	0.557 <sup>a</sup>
$^{40}\text{Ca} + ^{124}\text{Sn}$	1000	3.766 <sup>a</sup>	0.544 <sup>a</sup>	5.490 <sup>b</sup>	0.534 <sup>b</sup>
$^{28}\text{Si} + ^{208}\text{Pb}$	1148	3.140 <sup>b</sup>	0.537 <sup>b</sup>	6.631 <sup>a</sup>	0.505 <sup>a</sup>
$^{40}\text{Ar} + ^{165}\text{Ho}$	1206	3.530 <sup>b</sup>	0.542 <sup>b</sup>	6.180 <sup>b</sup>	0.570 <sup>b</sup>
$^{32}\text{S} + ^{232}\text{Th}$	1440	3.374 <sup>a</sup>	0.558 <sup>a</sup>	6.7915 <sup>b</sup>	0.571 <sup>b</sup>
$^{48}\text{Ti} + ^{208}\text{Pb}$	1804	3.843 <sup>b</sup>	0.588 <sup>b</sup>	6.631 <sup>a</sup>	0.505 <sup>a</sup>
$^{56}\text{Fe} + ^{208}\text{Pb}$	2132	4.106 <sup>b</sup>	0.519 <sup>b</sup>	6.631 <sup>a</sup>	0.505 <sup>a</sup>
$^{64}\text{Ni} + ^{208}\text{Pb}$	2296	4.212 <sup>b</sup>	0.578 <sup>b</sup>	6.631 <sup>a</sup>	0.505 <sup>a</sup>
$^{70}\text{Zn} + ^{208}\text{Pb}$	2460	4.409 <sup>b</sup>	0.583 <sup>b</sup>	6.631 <sup>a</sup>	0.505 <sup>a</sup>

(a) Based on the 2PF profile extracted from [27]

(b) Based on the 2PF profile extracted from [31]

Table II. The calculated values of  $b_i$  constants, Eq. (12), for each of the considered versions of the M3Y interactions.

M3Y-version	$b_0$	$b_1$	$b_2$	$b_3$	$b_4$
DDM3Y1	-4.60490	3.95512	-1.25831	0.17061	-0.00801
CDM3Y3	-4.76641	4.18392	-1.38053	0.19862	-0.01310
BDM3Y1	-5.76935	5.59630	-2.11432	0.36185	-0.02335

Table III. The  $\chi^2$  values caused by imposing various physical effects on the barrier heights calculated by the Prox. 77 for our considered mass range.

Proximity model	$\chi^2$
Prox. 77	5.215
IPM1	3.270
IPM2	2.878
IPM3	2.621
Prox. 77 (BDM3Y1)	1.438

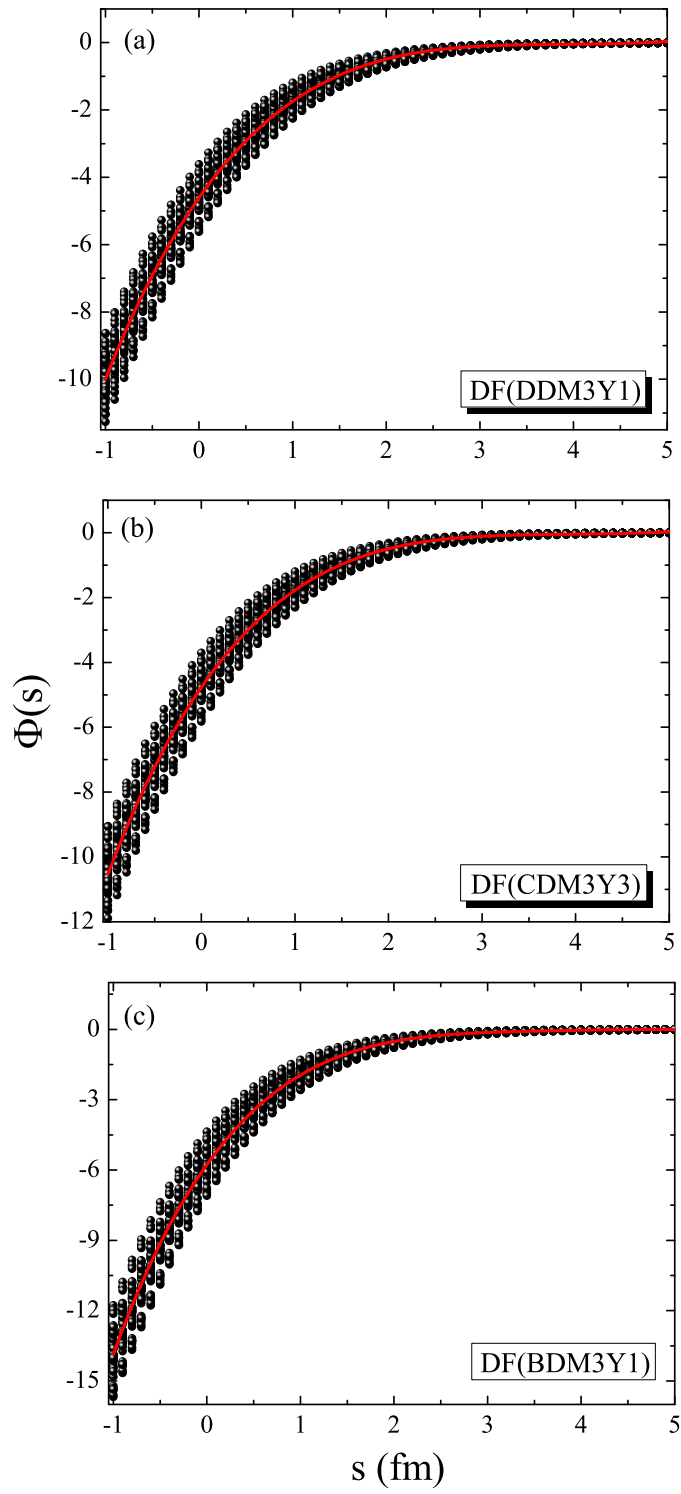


Figure 1:

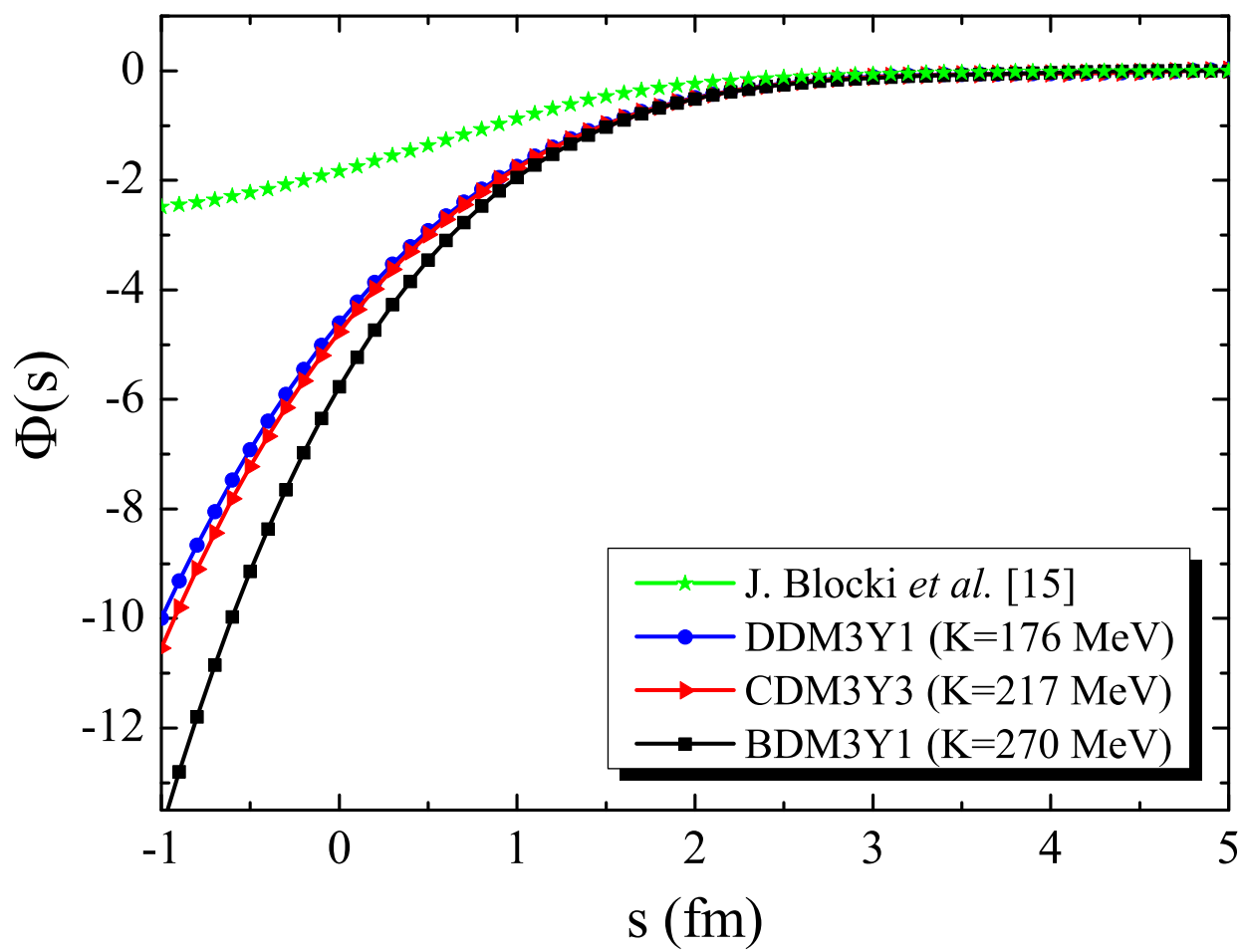


Figure 2:

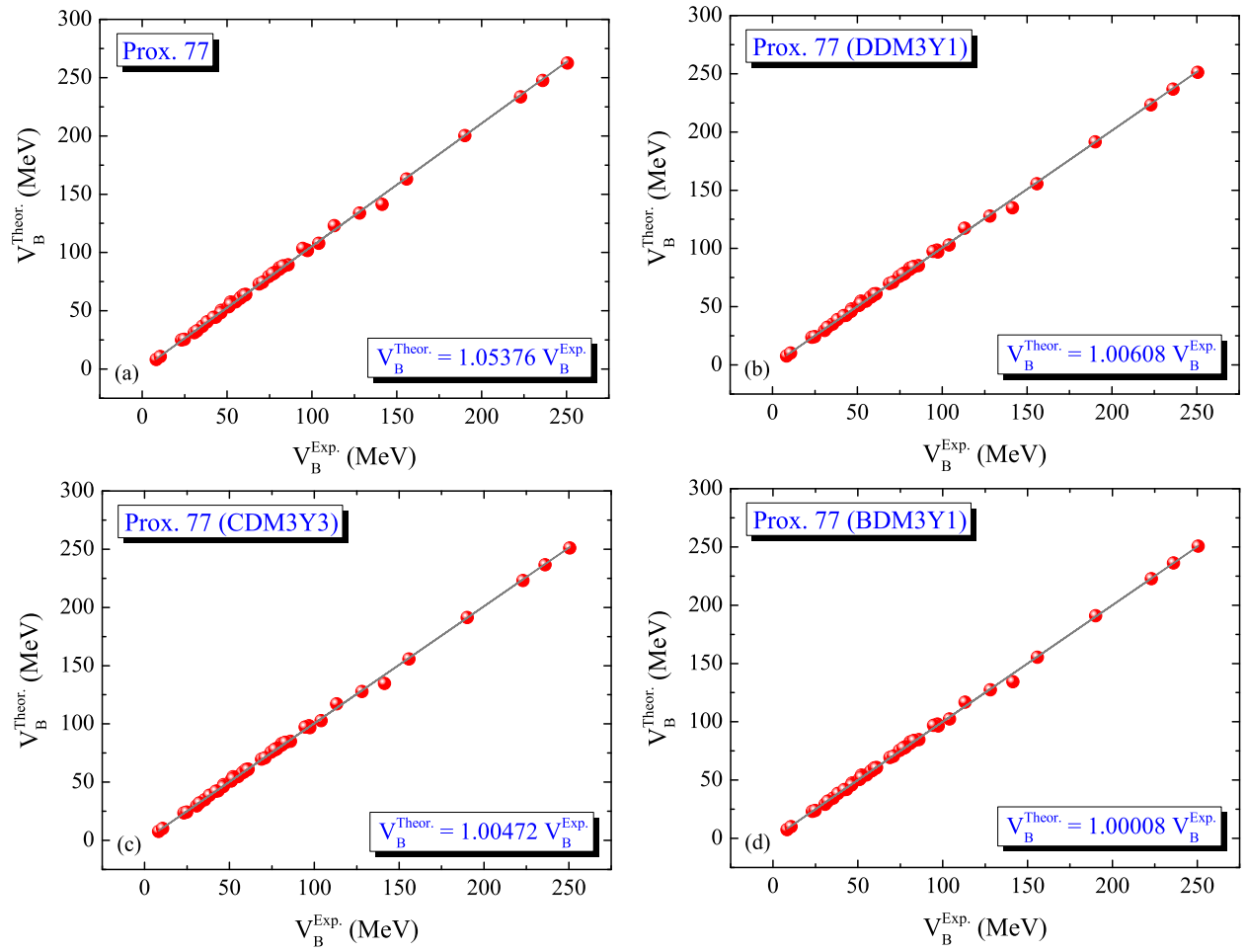


Figure 3:

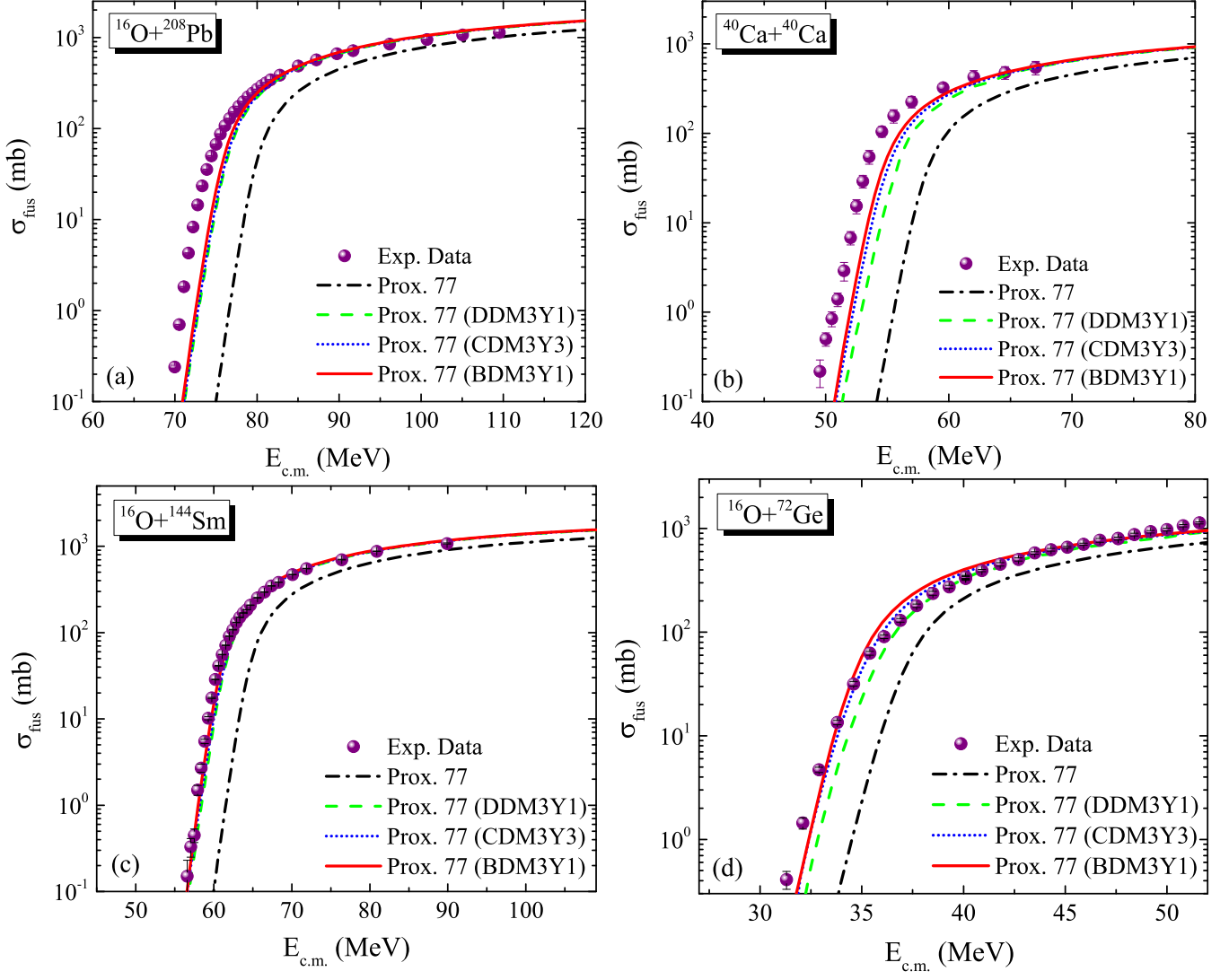


Figure 4:

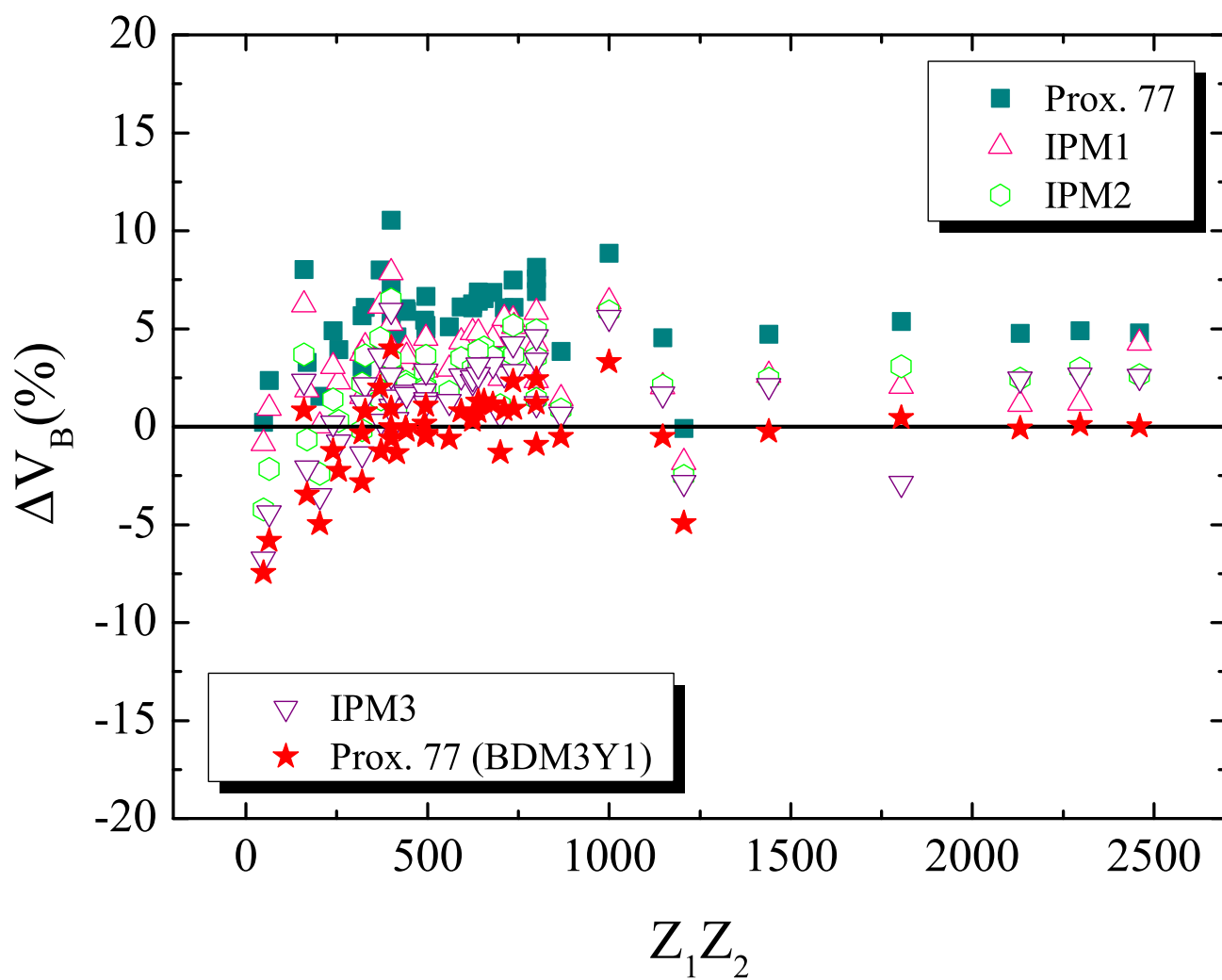


Figure 5:



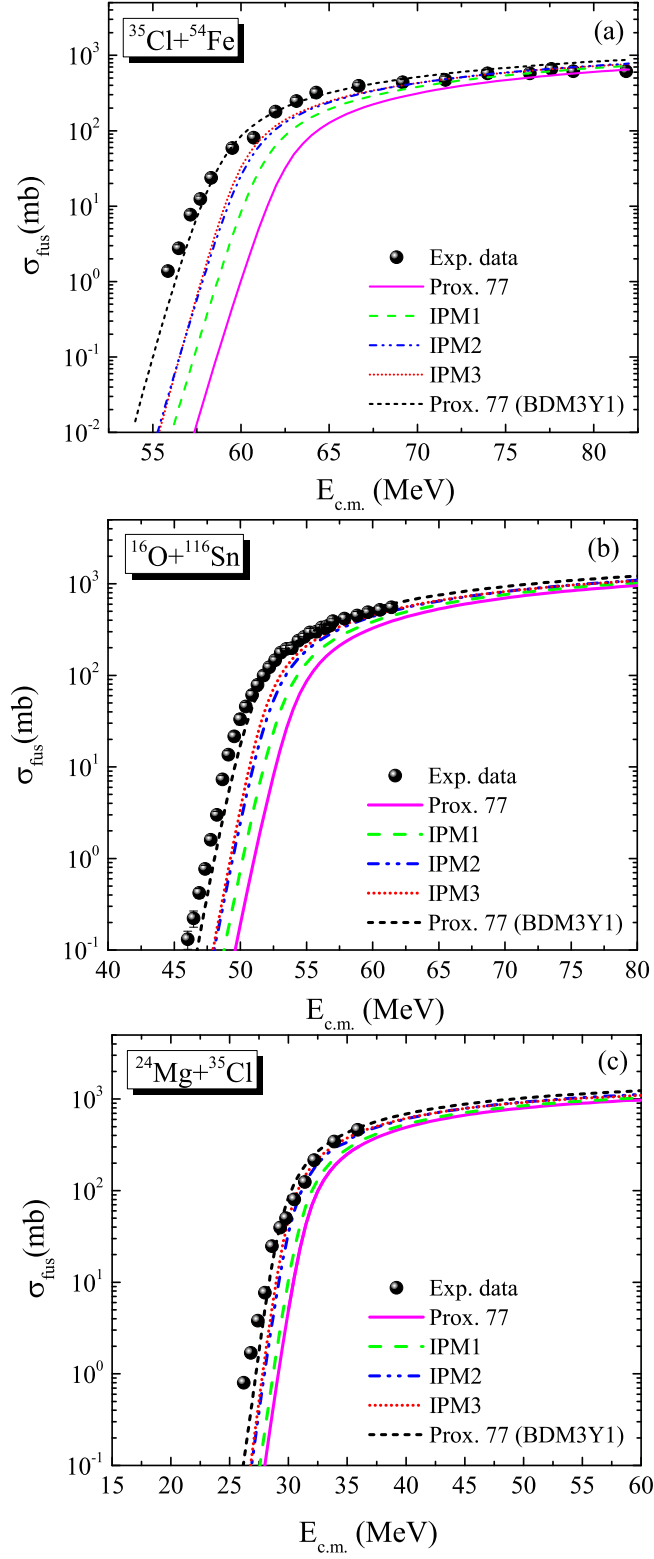


Figure 6: